Titanium-Indiffused Lithium Niobate Waveguide Fabry-Perot Modulator

By
Nabila Farhin Jahan
Mentor: Satsuki Takahashi

McNair Summer Research Program
May 27 – July 22, 2009

Abstract:

Because of its sensitivity to electric fields and ability to withstand electromagnetic pulse attacks, Titanium indiffused Lithium Niobate waveguide has been a reasonable choice to use as a Fabry-Perot resonant modulator in non-metal radio frequency receivers. In this paper, the device demonstration of a previously fabricated Titanium indiffused Lithium Niobate waveguide is discussed, alone with a brief discussion of the use and the fabrication process of the device. Due to power loss, the intensity of the laser light output through the device becomes significantly lower than the input, which deteriorates the performance of the device. In order to measure the performance of the device as a Fabry-Perot resonator, the power loss is observed, and the laser light output intensity vs. wavelength spectrum is analyzed in comparison to the theoretical spectrum of an ideal Fabry-Perot resonator of similar features.

Introduction:

In today's world, high power electromagnetic weapon sources impose a rising threat to modern electronics made of metal interconnects and circuitry. Any powerful electromagnetic pulse attack has the ability to destroy or permanently damage the metal interconnects and sensitive electric circuitries in the currently available devices. The Graham Commission report presented to the U.S. Congress' House Committee on Armed Services in 2004 acknowledged the vulnerability of the available electronic systems and recognized the need to design devices having less susceptibility to such threats (Hsu et al., 2007). The risk of this kind of damages intensifies farther in case of radio frequency (RF) receivers where the antenna provides a direct entrance for the damaging electromagnetic radiation into the device.

Therefore, a new RF receiver structure has been proposed which will eliminate all metal interconnects or wiring and instead use dielectric or electro-optic materials as the RF receiver front-end. The device will contain three main parts – a dielectric receiver antenna (DRA) which will store the received radio waves, an electro-optic waveguide modulator (situated inside the DRA) which will carry laser light and modulate it using the electric field created by the radio waves, and a conventional photo detector at a farther distance which will convert the modulated laser light waves into electric signals and send them to a signal processing device.

The proposed project is a joint project by UCLA and USC electrical engineering/electrophysics research groups. The UCLA research group took interest in building the DRA, while the USC research group is taking part in building the electro-optic resonant waveguide modulator. The proposed waveguide modulator will be made

with Titanium indiffused Lithium Niobate crystals, a suitable electro-optic material to match the desired properties of the proposed device.

Characteristics and Purposes of the device:

The characteristics of the proposed RF receiver will mainly be three fold: complete absence of metal interconnects to increase the device's ability to withstand electromagnetic pulse attacks, charge isolation to farther strengthen the device by electrical-optical-electrical conversion, and device size reduction to ease the use and transportation of the device. (Hsu et al., 2007)

The characteristics of the waveguide modulator include it having a large electro-optic co-efficient, a low propagation loss and a reasonable purchasing or fabricating expense; Lithium Niobate in this case is the suitable choice (Takahashi, 2009).

Devices like X-band receivers have been used for military purposes (such as satellite communications and target identifications), and atmospheric measurements for weather forecasting. The newly proposed device have never been fabricated or used before. It might be used in a similar manner.

Literature Review:

The modern trend of weapon designing is very likely to aim toward weapon structures that are able to produce power transient surges capable of damaging sensitive circuits in electronic systems. On the other hand, modern tendency toward smaller sized circuits with smaller voltage tolerance makes electronics more vulnerable to such damage by strong electromagnetic radiation. In radiofrequency communication systems the antenna is a direct way for electromagnetic radiation to enter the device which puts the device at a higher risk. All these reasons give rise to the idea of a radiofrequency receiver

front end featuring a complete absence of metal electronic elements. The proposed device would be “a new type of RF receiver featuring absolutely no metal electrodes, interconnects and transistors in the front end” (Hsu et al., 2007), containing a dielectric resonator antenna and an electro–optic field sensor; By eliminating the soft spots of a conventional receiver, the new technology is aimed at addressing the vulnerability of today’s wireless communication and radar systems” (Hsu et al., 2007). This device also reaches the goal of reducing the size of RF front end receivers for the convenience in use and transportation. (Hsu et al., 2007)

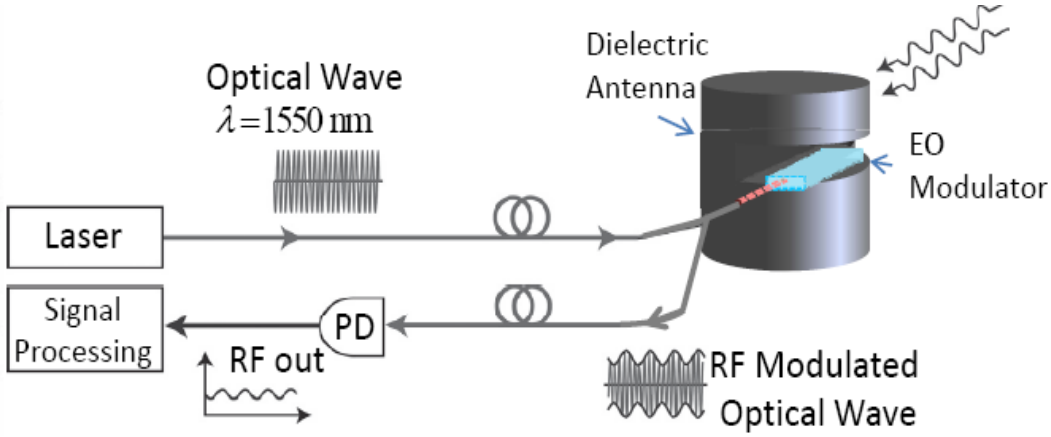

Figure 1: Device parts and operation. (Takahashi, 2009)

The main concept of this photonic-assisted all-dielectric RF front-end is to have two main parts built of dielectric and electro-optic materials – a RF receiver antenna and an optical resonator. Figure 1 refers to the structure of the device. The dielectric resonator antenna (DRA) gathers and concentrates the incoming electromagnetic field. The electromagnetic (EM) signal excites the resonance of DRA and a mode field pattern is built up inside the structure. The best location to put the Electro-optic (EO) resonator is at the location of the peak field intensity inside the DRA. The received EM signal is then delivered onto the optical resonator as a modulated optical signal by the antenna. The

signal is then carried through an optical fiber to a farther location where the signal is converted back to an RF signal which is then processed through various standard techniques (Hsu et al., 2007). “This front-end design significantly increases the threshold for damage associated with high power microwave signals. The lack of metal interconnects eliminates the one source of failure. In addition, the charge isolation provided by the optical link protects the electronic circuitry. Good sensitivity can be achieved due to signal enhancement provided by the microwave resonance in the DRA and optical resonance in the E-O resonator.” (Ayazi et al., 2007)

Although a conventional photo-detector (PD) is used in one part of the device in the signal path, it is isolated by the optical sensor from the air interface and the RF receiver following the idea of charge isolation to prevent damage caused by the EM waves. (Ayazi et al., 2007)

Although much work has been done on creating a fast sampler for electrical transients by sending short laser pulses through a $LiNbO_3$ crystal which is exposed to the electrical signal, the present work is substantially different from electro-optic sampling through the use of the dielectric antenna and the continuous-wave laser modulation (Ayazi et al., 2007). The formation of titanium in-diffused lithium niobate low-loss slab and stripe waveguides has been extensively investigated since 1974 (Armenise, 1988), but “not much has been published on the characteristics and diffusion mechanism of these waveguides since they were first fabricated in 1974.”(Griffiths & Esdaile, 1984).

A research paper by M. N. Armenise on fabrication techniques of Lithium-Niobate waveguides states that when trivalent of tetravalent atoms such as Fe Cr and Ti are diffused on to $LiNbO_3$, an increase of both ordinary index and extraordinary index n_o

and n_e is generated. Ti among them yields a good light confinement with relatively large increase of both ordinary and extraordinary refractive indices. Also, Ti in-diffusion allows the fabrication of optical waveguides supporting both TE and TM modes (Armenise, 1988), which is why titanium in-diffused Lithium-Niobate waveguides are very much likely to have the characteristics necessary for the project.

One of the first researches done on Titanium in-diffused Lithium-Niobate fabrication was done by Grant J. Griffiths. His experiment involved y-cut waveguides fabricated from films radio frequency sputtered from a 15 cm 99.999 percent titanium target in an argon atmosphere at 7 mtorr and 300W. Diffusion furnace used had a dimension of 30 cm 0.5"C flat-zone, fitted with a 7.6 cm diameter Vitreosil glass furnace tube. Although this material is damaged by out-diffused LiO_2, some etching of the dedicated tube was acceptable. The lithium loss by out-diffusion in these experiments was not given much attention. High-purity nitrogen and argon-free oxygen gases were used. An accurate refractive index model was needed to determine the effects of the various fabrication parameters on guide characteristics in this research. The problem with this setting of waveguide is that the small refractive index change results in sparsely moded guides, which is inconvenient for the setting. Another major concern in the fabrication of optical waveguides is the poor surface finishes which causes scattering losses and degrades coupling efficiency. Incomplete diffusion results in a granular layer of titanium oxide remaining on the surface, and that this layer is difficult to remove by etching or other means. The degree of surface roughness was observed to decrease with time and increasing temperature during diffusions, suggesting that it is the intrusion of niobium into the surface layer from the substrate which produces the surface roughness.

No difference was observed between surfaces of guides diffused in oxidizing or inert atmospheres. In order to avoid the undesirable effects of poor surface finish it is recommended that guides be fabricated at temperatures between 1050 and 1150°C in air or pure oxygen. This reduces attenuation by reducing the surface roughness which decreases the chance of optical damage, and reduces the uncertainty in the waveguide refractive index profile arising from oxygen deficiency and unpredictable effects of re-oxidation. (Griffiths & Esdaile, 1984)

Diffusion of titanium thin layers in the experiment of M. N. Armenise was also carried out at a temperature 900 to 1150 degree in argon nitrogen oxygen or air ambient, for diffusion times ranging from 0.5 to 30 hours. (Armenise, 1988)

To attain the goal to decrease optical losses, in-plane scattering losses in Ti:$LiNbO_3$ waveguides should be taken care of (Armenise, 1988). The performance of the resonant structures of the waveguides depends on the waveguide attenuation. A number of methods have been developed to determine the waveguide losses. A research by R. Regener and W. Sohler demonstrated that “it is possible to use low-finesse waveguide Fabry-Perot resonators in Standard crystal orientations to evaluate the total loss of both polarizations. The measurement of the contrast of the resonances is sufficient to calculate a combined loss-reflection factor and thus an upper limit of the attenuation coefficient.” (Regener & Sohler, 1985). The resonator method proves to be especially valuable for characterizing samples which are to be used for a fabrication of high-finesse waveguide resonators. (Regener & Sohler, 1985)

Regener and Sohler conducted their experiment with a single frequency He-Ne laser as the light source. It was a necessary condition to reach their goal to either use

lasers with a single frequency or to correct the measured interference contrast dependent on the intensity ratios of the different longitudinal laser modes. They used Ti:LiNbO3 strip waveguide resonators of 43 mm length on a z-cut crystal, shaped and polished thoroughly, containing the in-diffusion of a 350A thick Ti-stripe of 3 pm width at 1060 degree Celsius for 9 hours. They measured the contrast K of the Fabry-Perot resonances in optical waveguide resonators to determine the combined loss-reflection factor and concluded that if the end-face reflectivities for the investigated mode are known, the waveguide attenuation coefficient can be evaluated. (Regener & Sohler, 1985)

M. N. Armenise suggests that further research should be done to see the relation between the optical properties such as mode number, mode index, field distribution, scattering levels, total attenuation, optical stability and structural properties such as homogeneity, defects, crystal quality etc. How the crystal compositions affect the optical characteristics and the waveguide fabrication should be more carefully researched. “Once this is known, reliable models for the waveguide formation may be derived. This is the key to improving reliability, stability and performance of integrated optic devices both in stripe and slab $LiNbO_3$ waveguides.” (Armenise, 1988)

Structure and Properties:

a) Dielectric Receiver Antenna:

The dielectric receiver antenna (DRA) in the RF receiver will have a cylindrical shape of 11.25mm diameter and 9mm height. The incoming radio wave will excite the resonance of the DRA causing a field pattern to be built inside the DRA. The Lithium-Niobate waveguide would be situated at the position of the peak field magnitude in order to obtain the maximum modulation (figure 2).

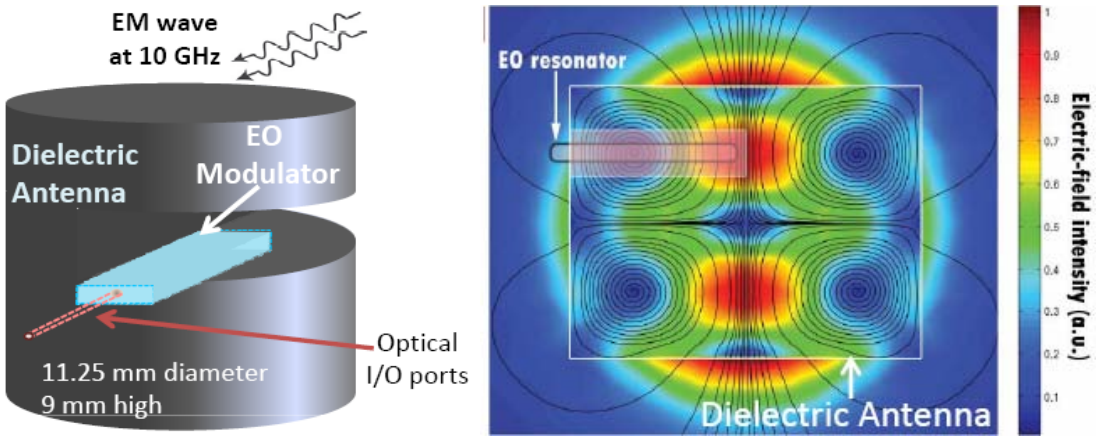

(a) **(b)**

Figure 2: (a) Dielectric Receiver Antenna, (b) four peak field magnitude inside the DRA. (Takahashi, 2009)

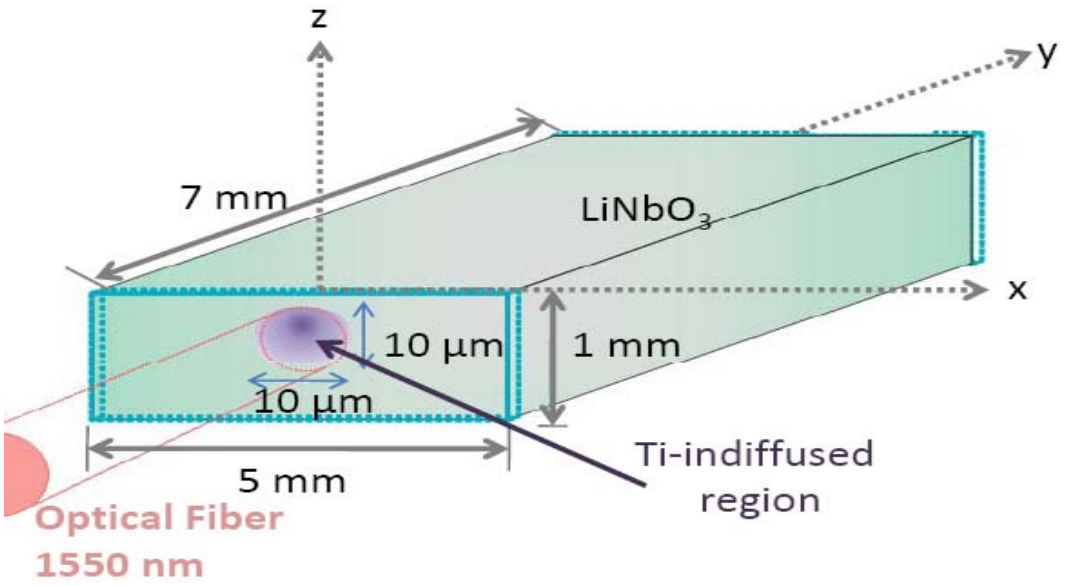

Figure 3: Titanium Indiffused Lithium Niobate Waveguide. (Takahashi, 2009)

b) Electro-optic (EO) resonant Modulator:

The Lithium Niobate substrate in the EO modulator has a rectangular shape with a 7mmX4mmX1mm dimension and the tunnel shaped Titanium waveguide has a diameter of 10 µm (figure 3). The targeted properties of the waveguide modulator are the following:

Sensitivity ~ 10^{-5} V/(mHz$^{1/2}$),

Targeted RF wave frequency and Free Spectral Range = 10 GHz and

Bandwidth = 100 MHz.

This particular EO resonant modulator would be a Fabry-Perot resonator type.

Fabry-Perot Resonatant Modulators (theory):

The waveguide will behave as a Fabry-Perot resonator. The waveguide cavity will have two partially transmitting mirror on the two end edges (figure 4). Light falling on the first mirror is partially reflected and partially transmitted. The transmitted light then goes to the second mirror and is again partially transmitted and partially reflected.

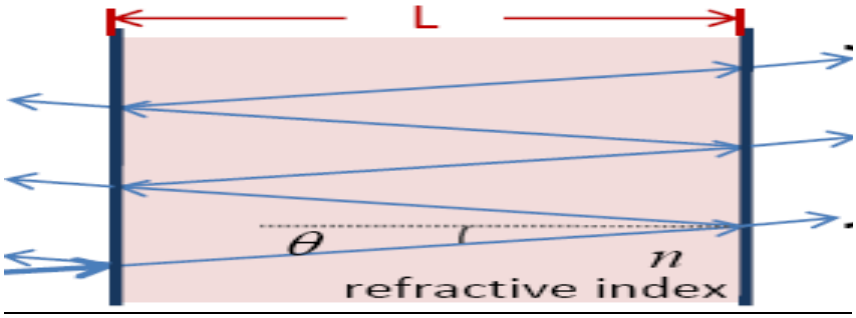

Figure 4(a): Fabry-Perot resonance inside the waveguide

It is best to make the light to enter the waveguide in zero degree angles (figure 4(b)) to ensure least propagation loss and most intensity output.

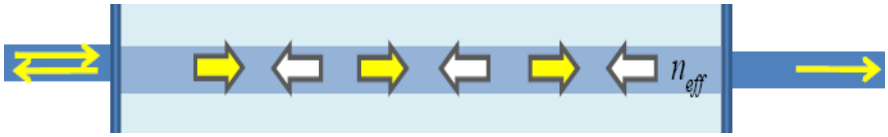

Figure 4(b): Fabry-Perot resonance when incident angle = 0 degree

The total reflected and transmitted power intensities can be represented by the following two equations respectively:

$$\frac{I_r}{I_i} = \left[\frac{\left(r_1 - r_2 e^{-2\alpha L}\right)^2 + 4 r_1 r_2 e^{-2\alpha L} \sin^2(\delta/2)}{\left(1 - r_1 r_2 e^{-2\alpha L}\right)^2 + 4\left(r_1 r_2 e^{-2\alpha L}\right)\sin^2(\delta/2)} \right] \qquad \frac{I_t}{I_i} = \left[\frac{\left(1 - r_1^2\right)\left(1 - r_2^2\right) e^{-2\alpha L}}{\left(1 - r_1 r_2 e^{-2\alpha L}\right)^2 + 4\left(r_1 r_2 e^{-2\alpha L}\right)\sin^2(\delta/2)} \right]$$

Here,
I_i = initial intensity, I_r = reflected intensity, I_t = transmitted intensity,

r_1 = reflectivity of mirror 1, r_2 = reflectivity of mirror 2, L = length of waveguide,

δ = phase change, α = propagation loss.

I_i (the initial laser light intensity), r_1, r_2 (properties of the mirrors) and δ (phase change) are fixed quantities in our case.

The followings are the representation of the above equations in 'intensity vs. mode' graphs (generated by a Matlab program). These graphs represent the occurrence of Fabry-Perot resonance inside the waveguide cavity.

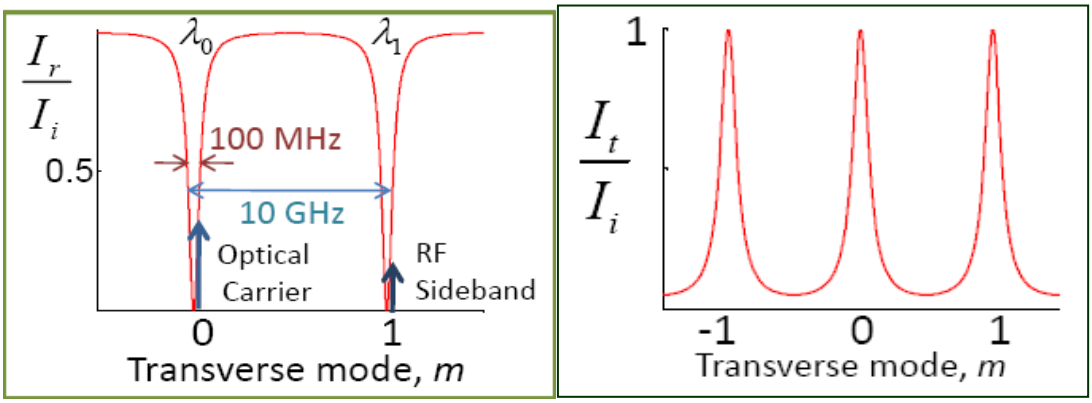

(c) **(d)**

Figure 5: Intensity vs. wavelength spectrums for reflected (c) and transmitted (d) light waves. (Takahashi, 2009)

Our goal is to observe the output 'intensity vs. wavelength' graph from the optical spectrum analyzer while we let light pass through the waveguide and check how well the graph shows resonance inside the cavity. The expected graph should have the following Properties (Takahashi, 2009) (figure 5(c)):

Free Spectral Range, FSR = 10 GHz (to accommodate 10GHz incoming radio wave frequency),

Bandwidth $\Delta\nu_{1/2}$ = 100 MHz,

(The length of the waveguide was determined by the targeted FSR value from the equation, $L = c / (2.n_{eff.}FSR)$ = 7mm, where c = speed of light, n_{eff} = effective refractive index in Lithium Niobate)

Research Methods:

A) Fabricating the z-cut, y-propagating Titanium in-diffused Mg-doped Lithium Niobate waveguide (done by Satsuki Takahashi):

A layer of titanium is deposited onto the LiNbO3 substrate. Then the samples are diced to sizes of 2cm x 2cm. Photoresist is spun on top of titanium. The waveguides are defined photolithographically, by UV exposing the photoresist with a mask placed above it. Then the substrate is placed in the photoresist developer solution, leaving behind the portion of the photoresist that defines the waveguide. Then the substrate is again placed in titanium etchant to remove all unwanted titanium. The remaining photoresist is removed with the photoresist stripper solution.

Now the samples are placed in a high-temperature quartz tube furnace and heated in 1000-1100 degree Celsius at a set rate of 4-6 degree per minute while Argon and Oxigen gas passing through water bubble is passed through the furnace.

The samples are diced with diced edges perpendicular to the waveguide axis and index distribution and effective index measurement is done. Final polishing of the edges is done in order to obtain a low-loss waveguide. (Takahashi, 2009)

B) Polishing the edges:

The final polishing of the waveguide edges should be as close to perfection as possible to minimize the power loss through the waveguide. Three diamond layered

circular polishing disks were used with the diamond sizes of 3 µm, 1 µm and 0.1 µm for hand polishing of the waveguides.

(a) **(b)** **(c)**

Figure 6: (a) Unpolished waveguide edges, (b) Diamond lapping polishing film, (c) Edge view after hand polishing.

Although the edge polishing looked fine under the microscope, it didn't produce a usable Fabry-Perot resonance spectrum. Therefore, several waveguides were sent out for commercial polishing to obtain the best results.

The polished waveguides have been tested before they were sent out again for mirror coding. The testing procedure is the following.

C) Device Demonstration: Obtaining Fabry-Perot Resonance Spectrum

A laser light of 1550 nm has been used to test the properly polished waveguide. The power of the laser light was measured to be 1mW before it was set to pass through the waveguide. The waveguide was then placed under a microscope to be visible and the center axis of an optical fiber carrying the laser light was aligned with the axis of the

waveguide to ensure proper light propagation through the waveguide. Next, a photo-detector was aligned with the axis of the waveguide to measure the power of the transmitted light coming out through the waveguide.

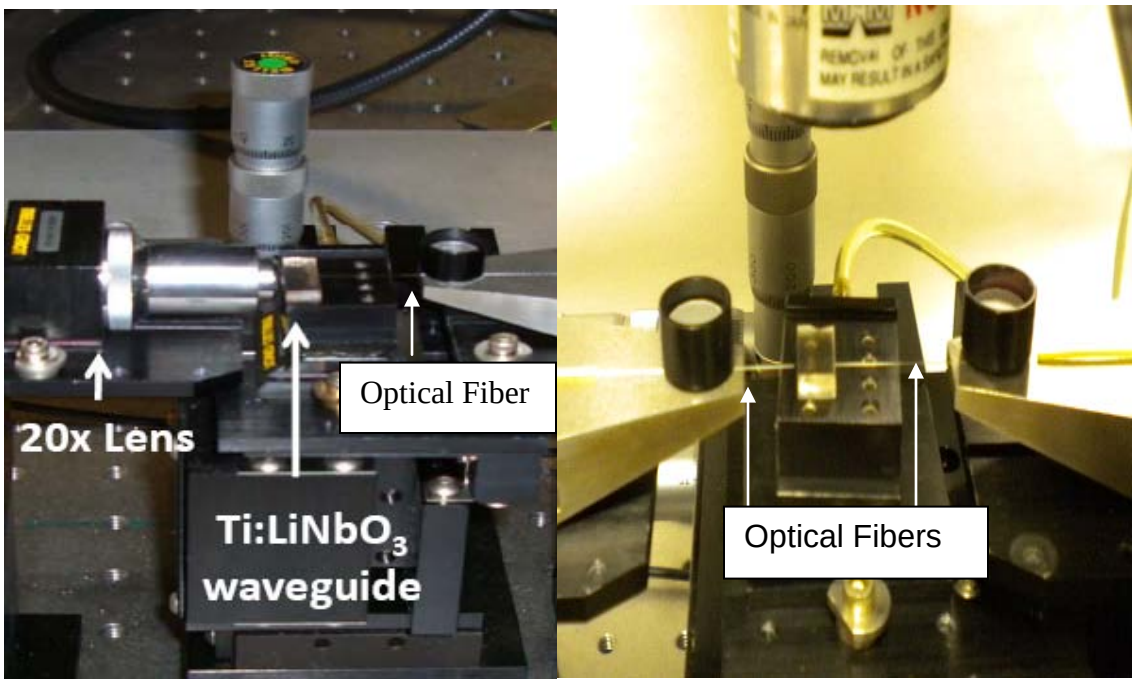

Figure 7: Alignment of the optical fibers with the waveguide edges under the microscope.

A second optical fiber is aligned with the other end of the waveguide so that the laser light now passes through it. The light looses more power through scattering and imperfect alignment. The other end of the second optical fiber is attached to an optical spectrum analyzer to obtain an 'intensity vs. wavelength' graph. The graph will be an indication of how well the Fabry-Perot resonance is happening inside the waveguide.

Measurements have been done on the obtained 'intensity vs. wavelength' spectrum to compare and fit it to a matlab generated Fabry-Perot resonant spectrum. Due to time constraint, only the depths of the obtained spectrums were analyzed and compared. Different propagation loss values (α) and mirror refractivity values (r_1, r_2) were plugged into the matlab program until the Fabry-Perot spectrum best fits the

obtained spectrum. (It is important to note that these waveguides have not been mirror coated yet.)

Results and Analysis:

The hand polished waveguide showed the following intensity (normalized) vs. wavelength spectrum (figure 8(a)):

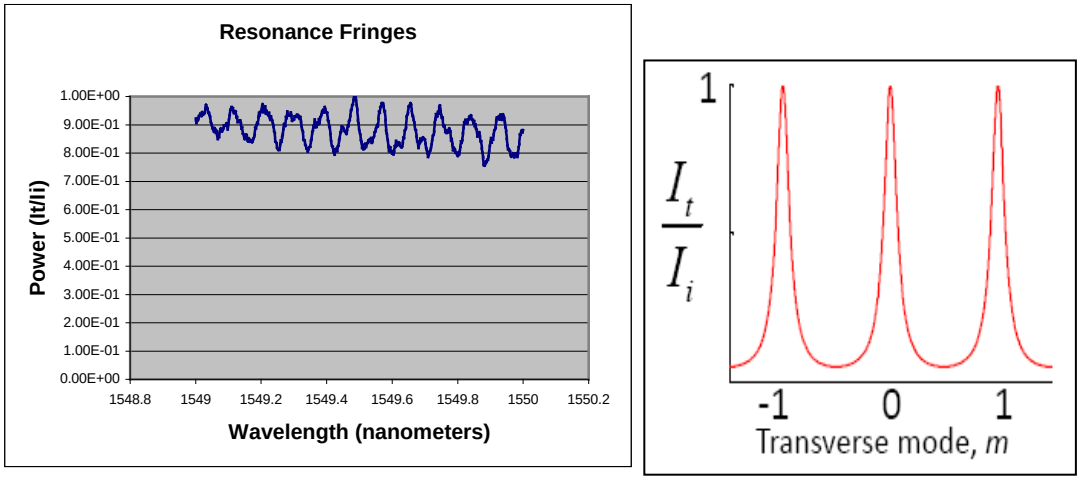

(a) **(b)**

Figure 8: (a) Spectrum of hand polished waveguide, (b) theoretical Fabry-Perot spectrum with no loss.

The spectrum does not look particularly good compared to the theoretical spectrum. No measurements were performed on this graph.

Out of 15 commercially polished waveguides, 9 waveguides gave usable results. The four best obtained spectrums are discussed in this section.

The best two 'intensity (normalized) vs. wavelength' spectrums are the following (figure 9):

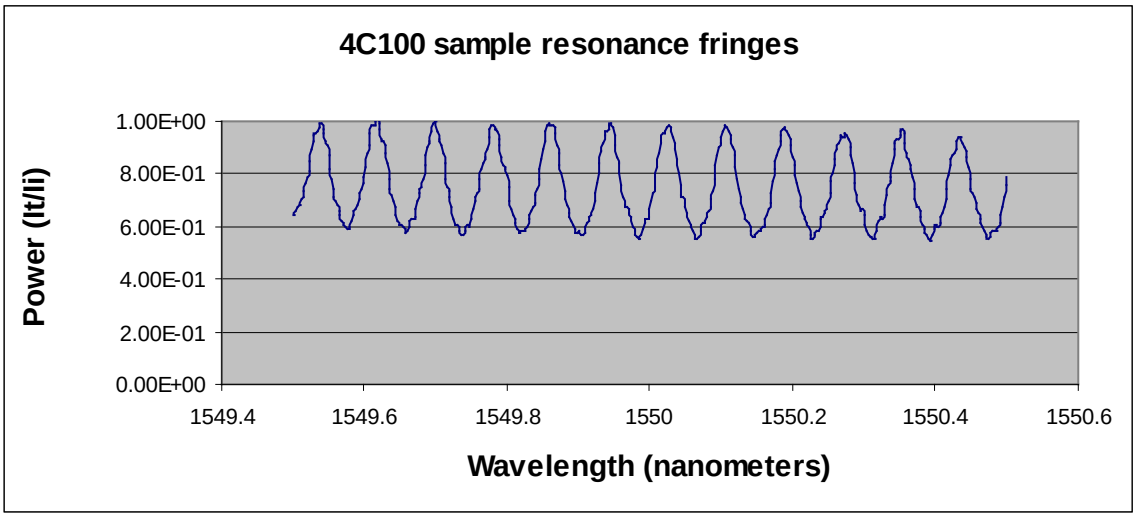

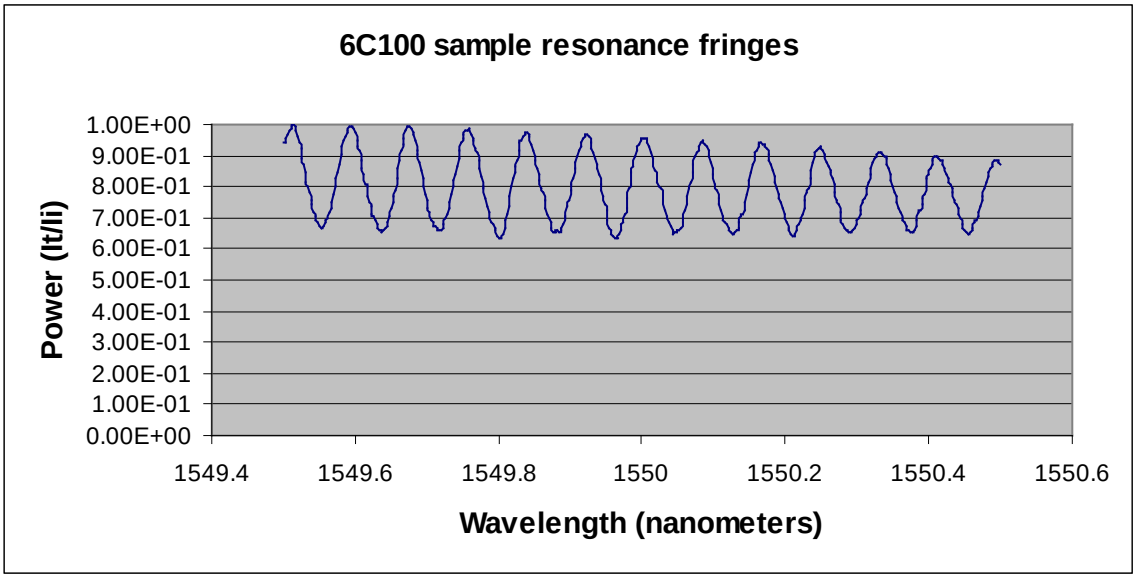

Figure 9: Spectrum from the best two edge polished waveguide samples.

The average depths (the distance between a peak and a trough) of the spectrums are,

For 4C100 sample, d ~ 0.4

For 6C100 sample, d ~ 0.3

The other two spectrums show a periodic variation in the intensity level (figure 10).

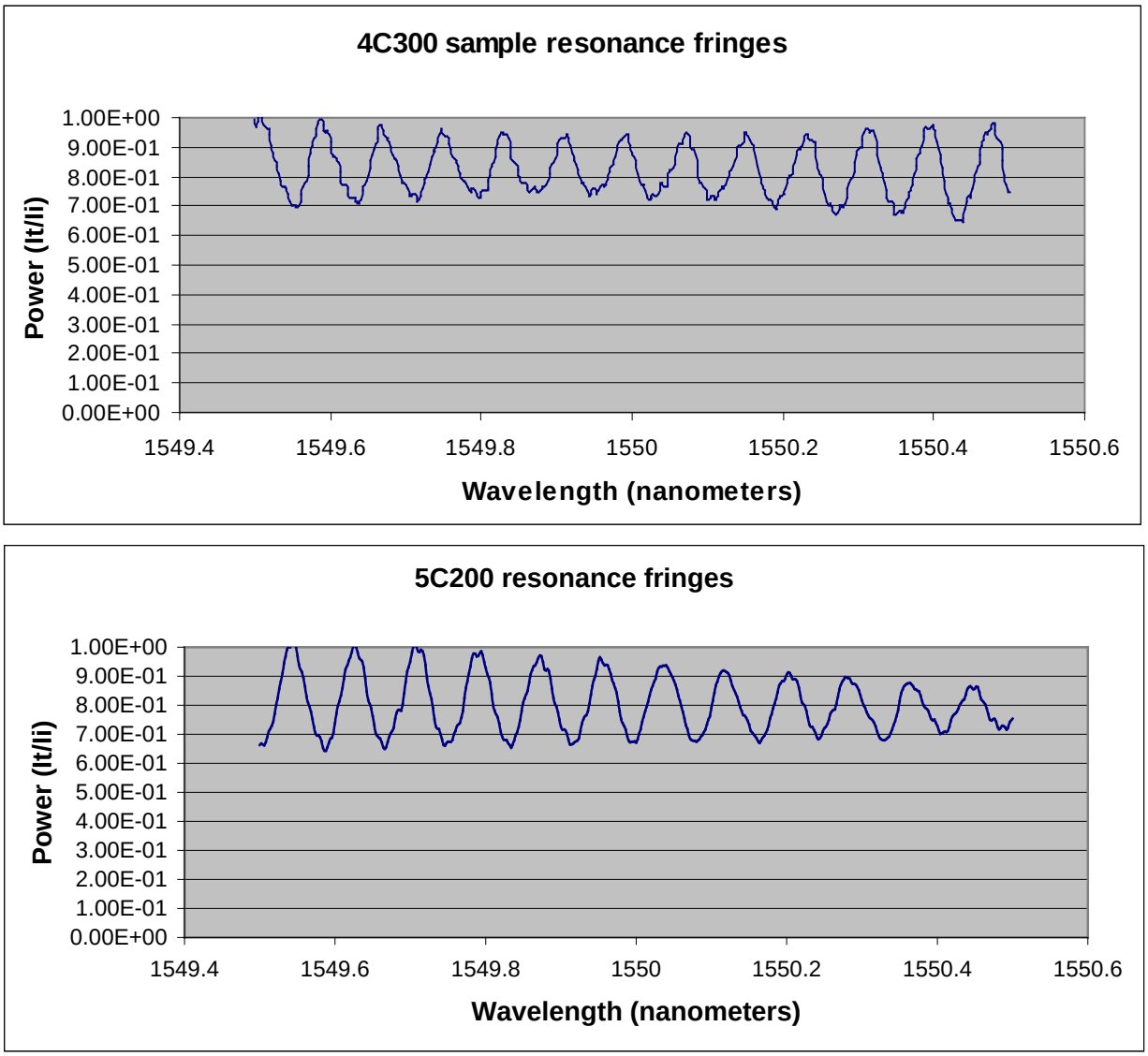

Figure 10: Intensity vs. wavelength spectrum from two edge polished samples.

The reason for the variation in intensity is unknown.

The average depths of the spectrums are,

For 4C300 sample, d ~ 0.26

For 5C200 sample, d ~ 0.27

Comparing with the standard graph:

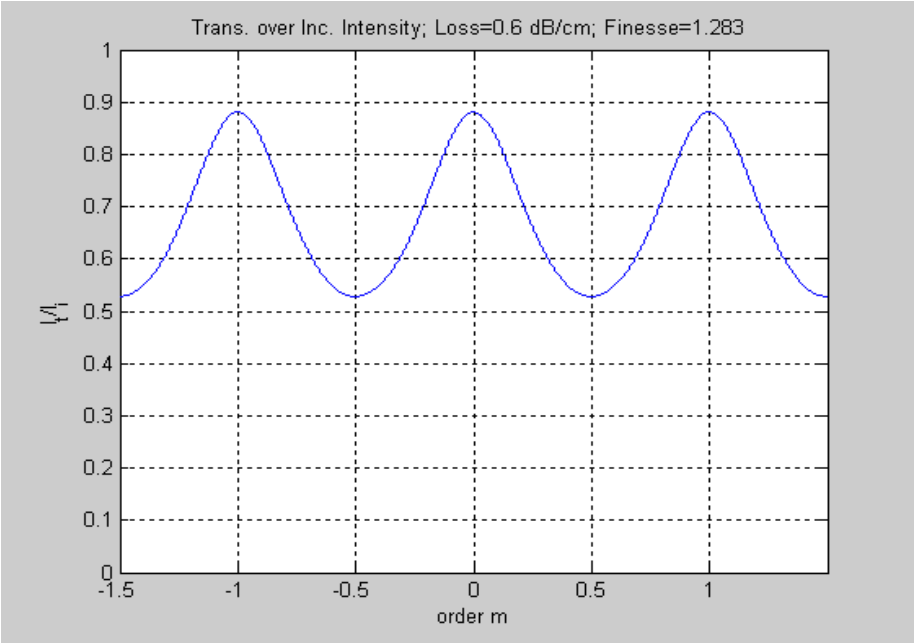

Figure 11: Matlab generated standard graph

Using our Matlab program we found a Fabry-Perot spectrum (figure 11) of similar depth (0.35) as the average depth of 4C100 and 6C100 samples by plugging in the $r_1=r_2=0.14$ (known reflectivity values for waveguide edges before mirror coating) and $\alpha=0.6$ dB/cm. Thus, we can assume that the samples will have a propagation loss value close to 0.6 dB/cm.

It should be noted that we are not performing measurements of the peak distances, FSR's, bandwidths and other properties of the resonance graphs yet. These measurements will be performed after the waveguide edges have been mirror coated.

Future Goals:

a) To develop a technique to properly polish the waveguide edges.

b) To continue repeating the process after the waveguide edges have been mirror coated to measure the quality and refractivity of the mirrors.

c) To find a way to reduce the propagation loss to a minimum.

d) To refine the resonance spectrum to match the theoretical Fabry-Perot resonant spectrum considering the minimum possible propagation loss

e) To find a way to analyze the maximum power output through the waveguide resonance modulator.

Conclusion:

If the above goals have been reached and a proper Fabry-Perot resonance is produced inside the waveguides, the waveguides will be sent to UCLA to be placed inside the dielectric receiver antenna. The performance of the waveguide under the influence of the dielectric RF antenna capturing radio waves will decide how successfully the whole device will perform as a radio frequency (RF) receiver. A successful electro-optic RF receiver featuring no metal interconnects or electrodes will highly reduce the risk of device damages caused by strong electromagnetic pulse waves during a nuclear attack, a very likely phenomenon to seriously consider in the post 9/11 world.

References

Armenise, M. N. (1988). Fabrication techniques of lithium niobate waveguides. *IEEE Proceedings*, 135J(2), 85-91.

Ayazi, A., Hsu, R., C. J., Houshmand, B., Steier, W. H., and Jalali, B. (2007). All-dielectric photonic-assisted wireless receiver. *Opt. Express*, 16, 1742-1747.

Griffiths, G.; Esdaile, R. (1984). Analysis of titanium diffused planer optical waveguides in lithium niobate. *IEEE Journal of Quantum Electronics*, 21(2), 149-159.

Hsu, R. C., Ayazi, A., Houshmand, B., and Jalali, B. (2007). All-dielectric photonic-assisted radio front-end technology. *Nature Photonics*, 1, 535-538.

Regener, R., Sohler, W. (1985). Loss in Low-Finesse Ti:LiNbO3 Optical Waveguide Resonators. *Appl. Phys*., B 36, 143-147.

Takahashi, S. (2009). Titanium-indiffused Lithium Niobate waveguide Fabry-Perot modulator. From PhD. qualifying examination paper, USC, Los Angeles.